東京大学 大学院新領域創成科学研究科
基盤科学研究系
先端エネルギー工学専攻

平成 23 年度

修士論文

Investigation of Laser Supported Detonation Structure Using Half Self-emission Half Shadowgraph Method

－HSHS 撮像法によるレーザー支持爆轟波構造の解明－

2012 年 2 月提出
指導教員　小紫　公也　教授

47106074　道上　啓亮

Contents

Table and Figure List

Chapter 1

Chapter2

Chapter 3

Appendix

CHAPTER 1
Introduction

1.1 Background

Recently, there is some concept as SSPS which needs large amount of transport to space. However, transportation by a traditional rocket using chemical fuel costs a great deal of money, thus it is unrealistic. This is because the chemical rocket needs large amount of on- board fuel and almost all of its expensive components are disposable.

Laser propulsion is a candidate for a low-cost launching system, and can be considered as the mass driver, in which the vehicle is accelerated by the laser power transmitted remotely from the ground-based or space-based laser.

1.2 Laser Propulsion System

The Laser propulsion system was first suggested by Kantrowitz[1)] et al, 10 years after the laser system had been innovated. At that time, the system was that the projectile gets the thrust by laser ablation. However, the Air breathing type of laser propulsion system can reduce the on board propellant, hence the Air breathing type had been studied actively. At the same time, some studies about Energy conversion process from laser to plasma and shock wave was done by Raizer[2)] et al. From the 1970s to the 1980s, studies were conducted on generating the high pressure region on the metal plate by atmospheric plasma induced by the irradiation of high power laser[3,4,5)]. After these, bell type nozzle projectile was developed and investigated experimentally by Pirri[6)] et al. This system has the parabolic mirror which focuses the laser beam and induces the laser plasma. The projectile can get the thrust from blast wave of the laser induced plasma.

Ageev[7)] et al performed experiment on parabolic type and corn type nozzle projectile using 5J pulsed CO_2 laser and performed fluid dynamics analysis inside the nozzle using Sedov's self-similar solution method. In 1998, Myrabo[8)] et al conducted the experimental launch demonstration using pulsed 10kW class CO_2 laser. Their laser propulsion system leveled off at 71m, this projectile is called the 'Light Craft'.

In addition, in Japan, Sasoh[9)] is studying on laser ablation type propulsion system called LITA (Laser In-Tube Accelerator).

1.2.1 RP Laser propulsion

Repetitively Pulsed (RP) laser propulsion uses the repetitively pulsed laser. Pulsed laser beam is focused on the on-board collector]. When the laser beam is focused, the gas is ionized. Then laser-induced plasma and blast wave is generated at the focus. The plasma supports the blast wave. This particular kind of blast wave is called Laser supported detonation (LSD) wave. The flow energy provides thrust for the projectile. The detail of the LSD wave and the impulse generation process are described in a later section.

In comparison with existent chemical rocket, RP laser propulsion launch system is preferred due to the fact that its system structure is less complicated and does not require a heavy on-board power source as the laser energy is transmitted from a base either located in space or on the ground.

RP laser propulsion system is launched through three modes (air-breathing mode, ramjet mode and rocket mode) as shown Fig.1.1

In early stage of launch, the projectile breathes in atmospheric air from its backward side into its nozzle. Then the gas taken into projectile is expanded explosively by focusing laser and is discharged through the backward side. This is air-breathing mode. During this mode, projectile gain thrust by laser and atmospheric air, so it does not need fuel.

When the velocity of the projectile is M=1 ~ 8, the mode changes to ramjet mode. In this stage, the air intake opens and air is drawn through the front part and compressed to compensate the reduction of the ambient pressure. In this mode, compared to the air-breathing mode, the time to exhaust and refill air in the nozzle is much shorter because the intake flesh air sweep away the high-temperature and low-pressure air toward the rearward of the vehicle. Thus, in this mode, the laser could send more high frequency.

In the last stage, the launching mode changes to rocket mode. When altitude of vehicle is too high for sufficient air intake, liquid hydrogen is used as the working fluid. The thrust generation system is same as other modes. The RP laser propulsion system could accomplish high payload ratio, since the liquid hydrogen fuel carried on-board is required only for the rocket mode.

When the projectile is in the atmosphere, it does not need fuel, hence the concept of I_{sp} is non-existent. The chemical rocket needs large amount of fuel to go to outer space. This gives the laser propulsion launch system a competitive advantage within the atmosphere.

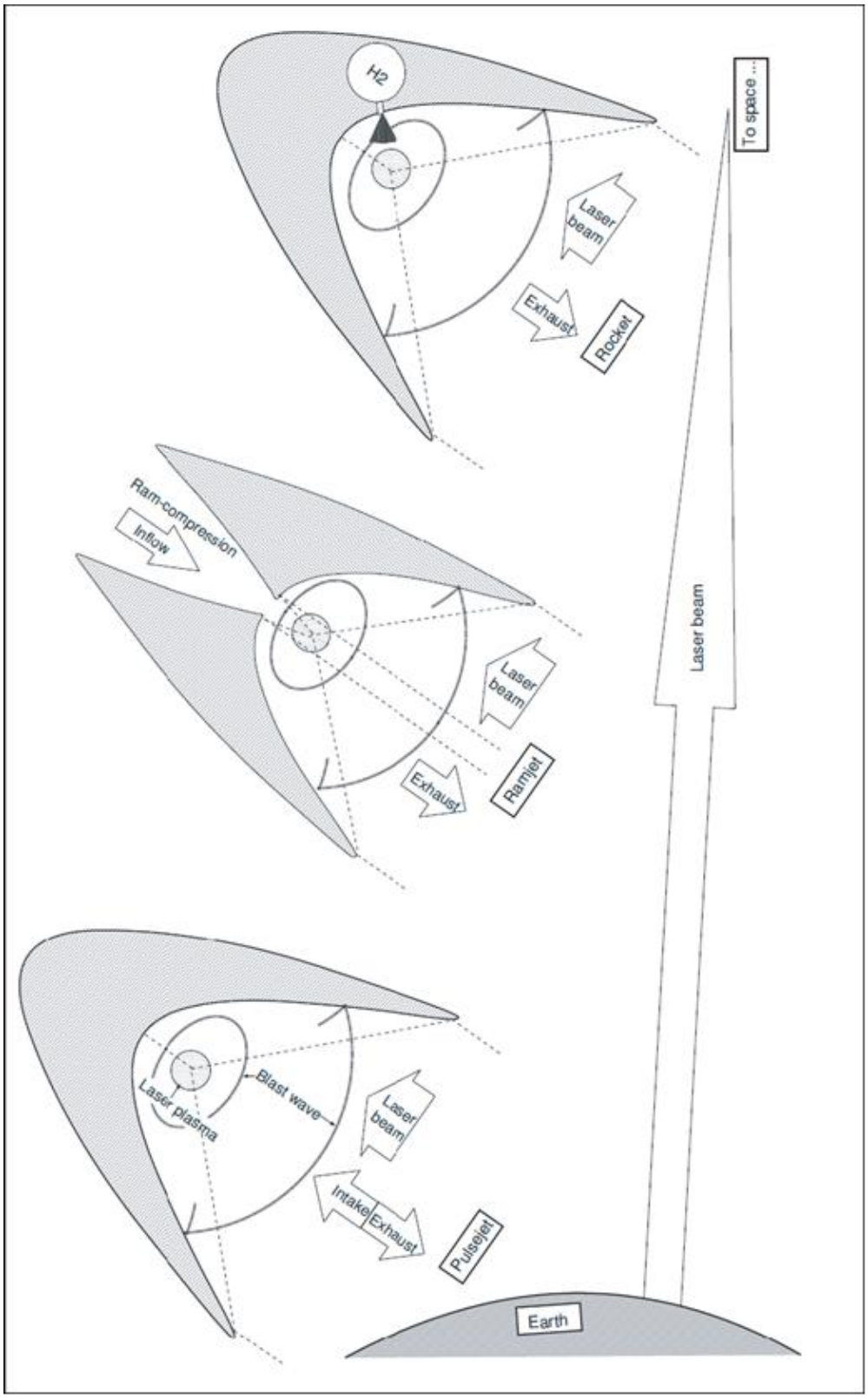

Fig.1.1 Laser propulsion launch mode

1.2.2 Impulse generation process

The impulse generation process of the RP laser propulsion could be divided into 4 steps as shown in Fig.1.2 and is as follows:

1. Breakdown of the gas and laser supported detonation (LSD) wave generation
2. Blast wave energy conversion
3. Impulse generation
4. Refill of the gas

In RP laser propulsion, the high power laser beam from the base located on the ground is focused on the projectile by its collector placed on its nozzle part and generates very high energy density region around the focusing area. When the energy density is enough high, a gas breakdown occurs and plasma is induced. The laser induced plasma expands drastically absorbing laser energy whiles being heated. The exponential expansion of the plasma compresses its ambient air strongly and a shock wave (blast wave) is induced. The plasma then drives the blast wave, and the blast wave energy is converted to the thrust work by a nozzle-shaped reflector[1,10]. As just described, the laser energy is absorbed and converted to the blast wave energy by the plasma in the laser supported detonation regime. The detail of the LSD[2] wave is described in the next section.

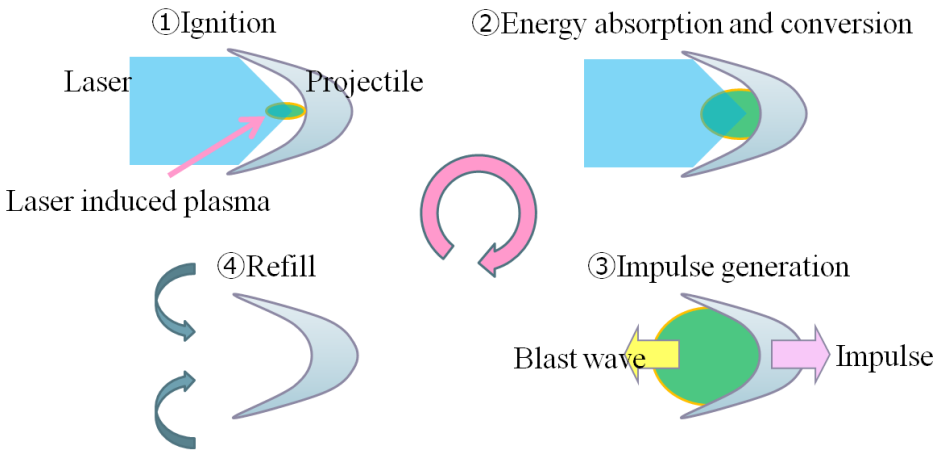

Fig.1.2 Impulse generation process

1.3 Laser Supported detonation

When a laser beam is focused, a gas breakdown occurs and plasma is induced. After that, the intense laser beam continues to be irradiated on the surface of the plasma. The laser energy is absorbed by this plasma mainly through the inverse-bremsstrahlung process[11]. When the laser power density is high enough in this absorption process, the plasma heats and compresses its ambient air. The plasma ionization wave travels at a supersonic velocity along the laser light channel in the direction opposite to the incident beam with a shock wave. This regime is called Laser Supported Detonation (LSD) wave. The laser absorption occurs in LSD wave[12,13,14]. On the other hand, when the laser power density is not enough to keep the LSD regime, the plasma ionization wave and shock wave are separated. This regime is called Laser Supported Combustion (LSC) wave. In the [LSC regime, the energy conversion from laser energy to blast wave energy is not achieved.

In Fig.1.3, a schematic of LSD and LSC are shown. Only the LSD regime can affect the energy conversion efficiency. However, a clear termination or a preservation mechanism and its exact structure are not elucidated physically. To understand the energy conversion efficiency, it is very important to investigate these phenomena.

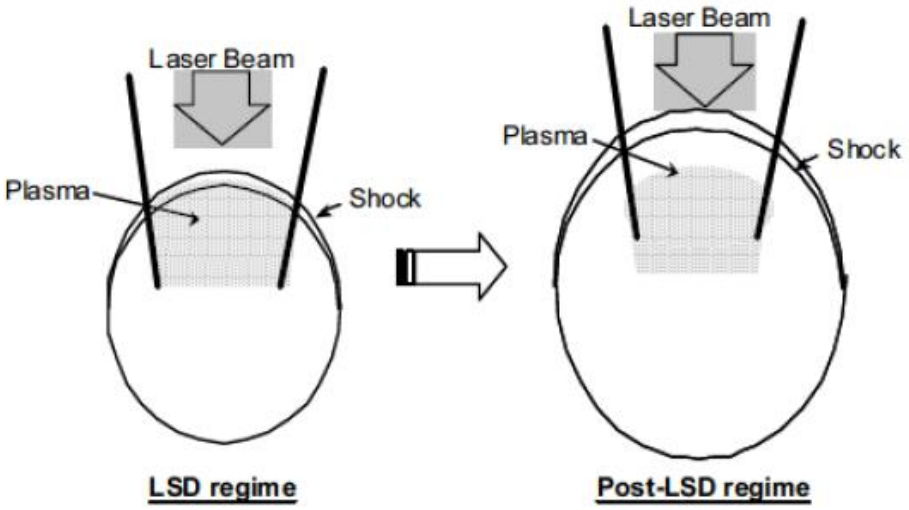

Fig.1.3 Schematic of LSD and LSC

1.4 Previous Study

Mori et al measured a blast wave induced by focused laser beam using Schlieren method as shown in Fig.1.4. They estimated the blast wave energy E_{BW} from the propagation history (Fig.1.5) of the shock wave and the ionization wave and evaluated the laser power density at the LSD termination S_{LSD}[15,16]. In addition, the energy loss by the plasma radiation was measured. This result is shown in Fig.1.6.

The relation between ambient gas pressure and E_{BW} is shown in Fig.1.7. Relation like this is reported in other researches[17,18]. This indicates that the E_{BW} is developed by ambient gas pressure condition.

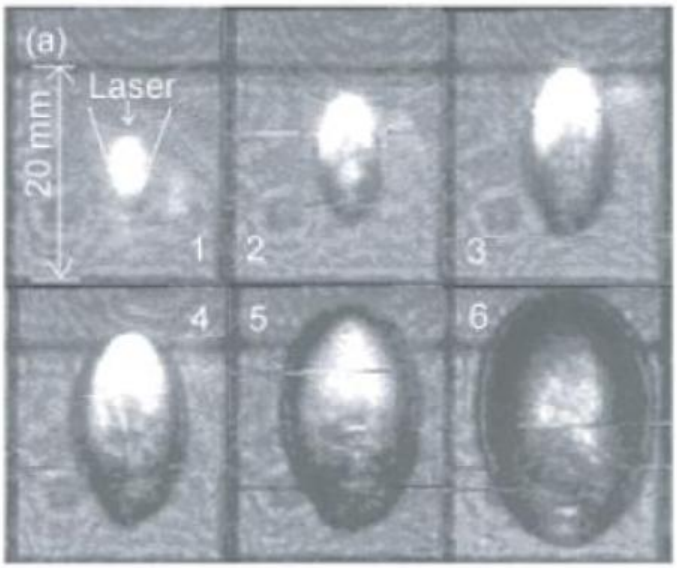

Fig.1.4 Schlieren image of blast wave

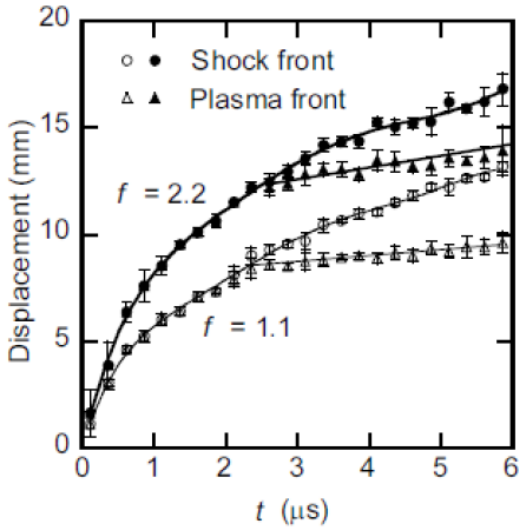

Fig.1.5 Propagation history

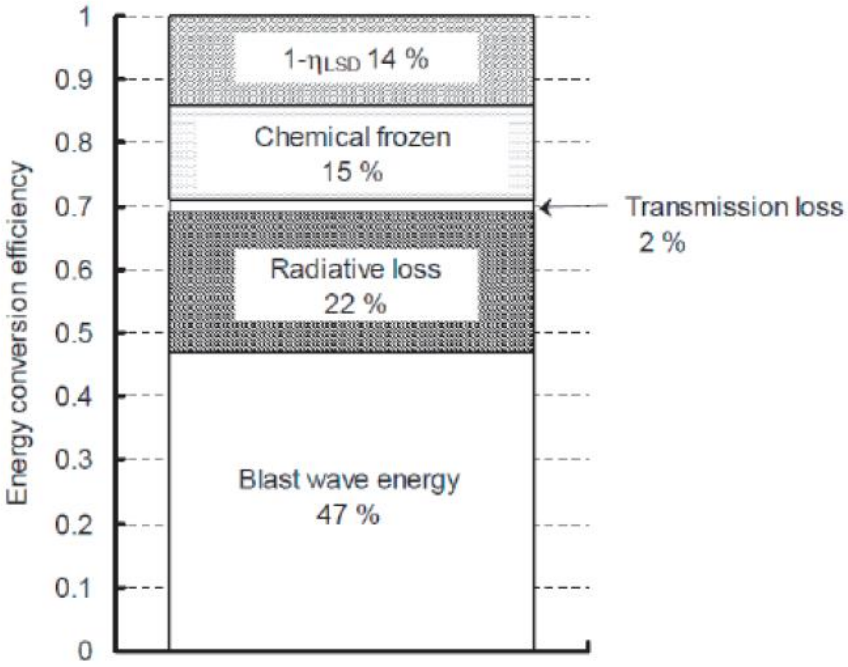

Fig.1.6 Blast wave energy conversion

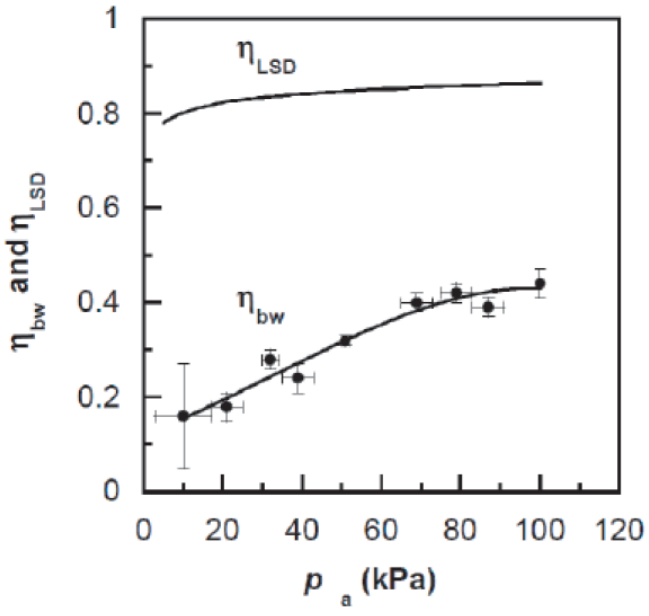

Fig.1.7 Relation between η_{BW} and the ambient pressure

Fkuda et al tried to elucidate the relation between the energy conversion efficiency and the electron number density by measurement of electron number density in LSD wave using Mach-Zehnder interferometry[19]. Their result showed that the peak of the electron number density behind the LSC wave was around 10^{24} m^{-3}]. However, the electron number density of LSD wave could not be measured because a strong radiation from the plasma disarranged the interference band (Fig.1.8).

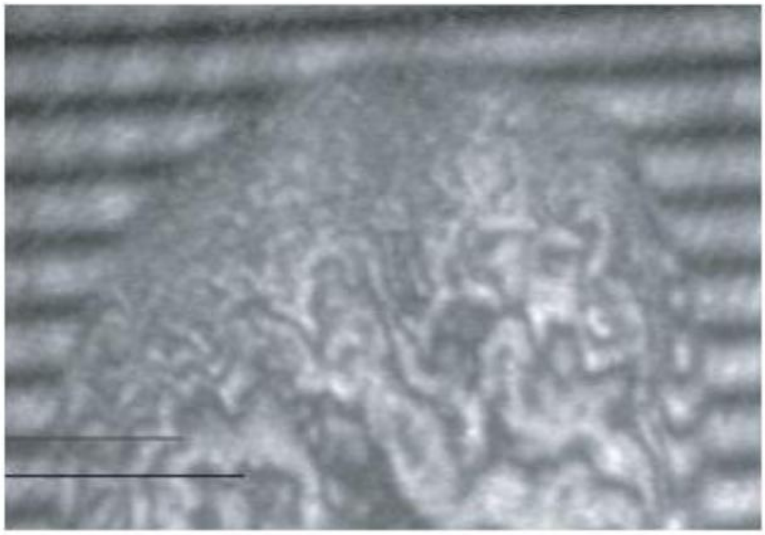

Fig.1.8 Image of interference band in LSD

Ushio et al investigated the line focused laser induced plasma[20]. When line focusing, the laser power density is not enough to cause breakdown. Therefore, the blast wave is generated by laser beam focused on aluminium plate, as shown in Fig.1.9. In addition, as shown in Fig.9, the walled blast wave was measured at the nozzle.

Fig.1.10 and Fig.1.11 show the images of 2-dimensions and quasi 1-dimension shadowgraph respectively as examples. Their propagation histories are shown in Fig.1.12 and Fig.1.13. From these, the blast wave energy conversion efficiency was calculated by self-similar analysis. The comparison with these results and point focusing blast wave results is described in Table.1.

Table.1 Characteristics comparison of the blast wave induced by each focusing conditions

Dimension Of Phenomena	2D	q1D	Point	
Focal Length / Beam Diameter	1.5	2.0	1.1	2.2
$\eta_{\mathrm{bw}}[\%]$	33	37	41	44
$t_{\mathrm{LSD}}[\mu\mathrm{s}]$	1.2	1.8	2.2	2.5
$S_{\mathrm{LSD}}[\mathrm{MW/cm^2}]$	3.4	1.7	2.6	3.7
M_{LSD}	5.3	6.3	5.3	5.4
$\eta_{\mathrm{LSD}}[\%]$	68	81	89	90
$\eta_{\mathrm{BW}}/\eta_{\mathrm{LSD}}[\%]$	49	47	46	49

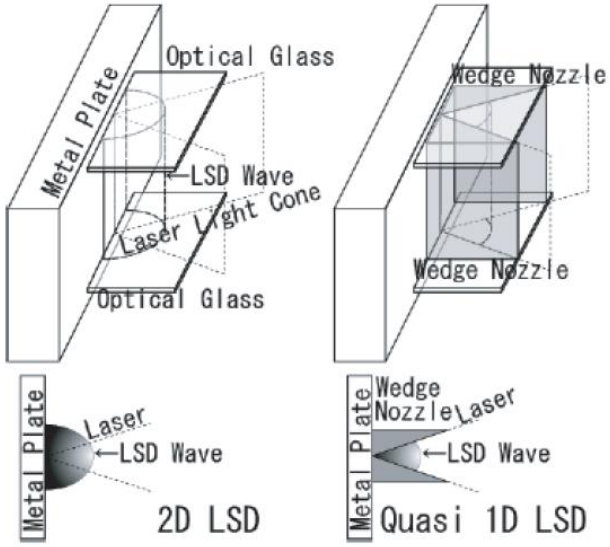

Fig.1.9 Schematic of 2-dimension and Quasi 1-dimension laser focusing system

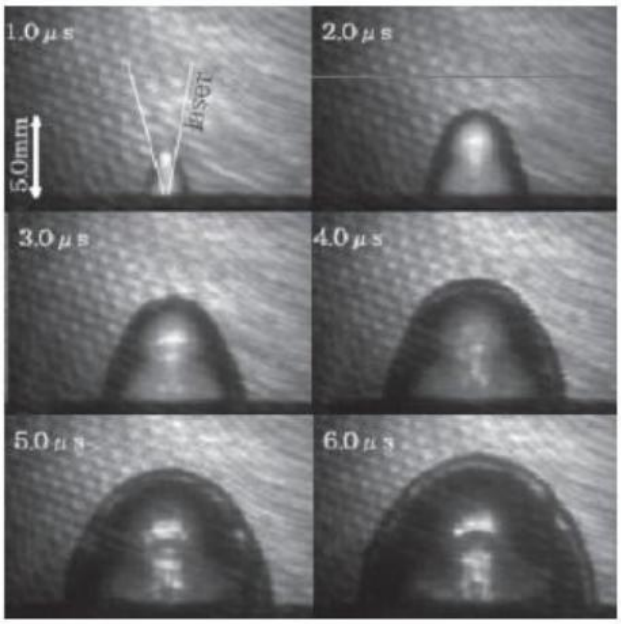

Fig.1.10 Image of 2-dimension laser plasma

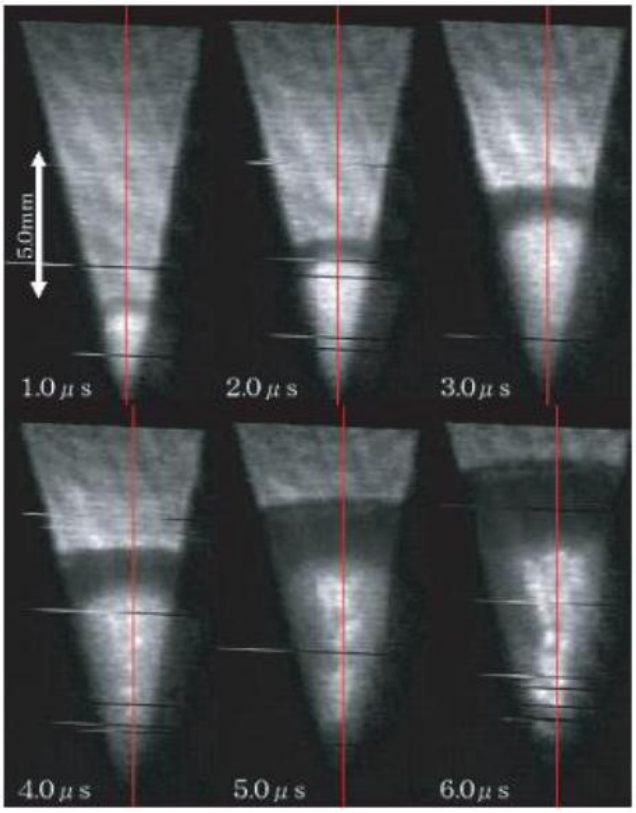

Fig.1.11 Image of quasi 1-dimension laser plasma

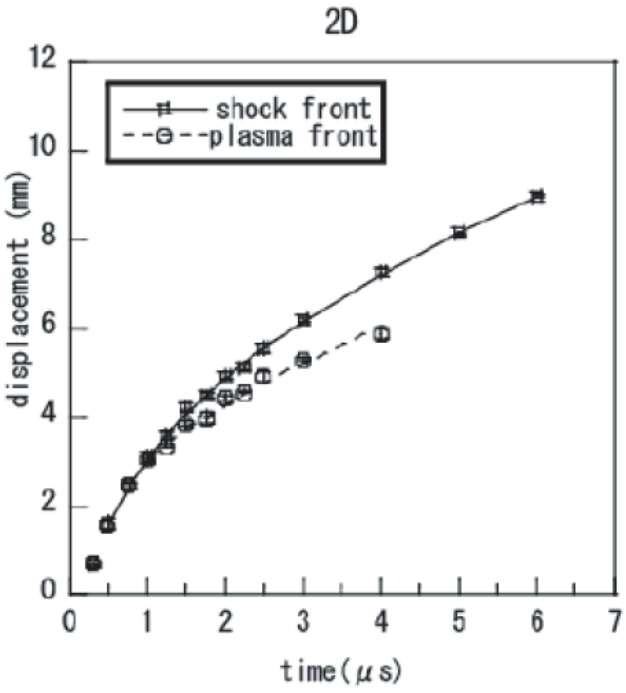

Fig.1.12 Propagation history of 2-dimension laser plasma

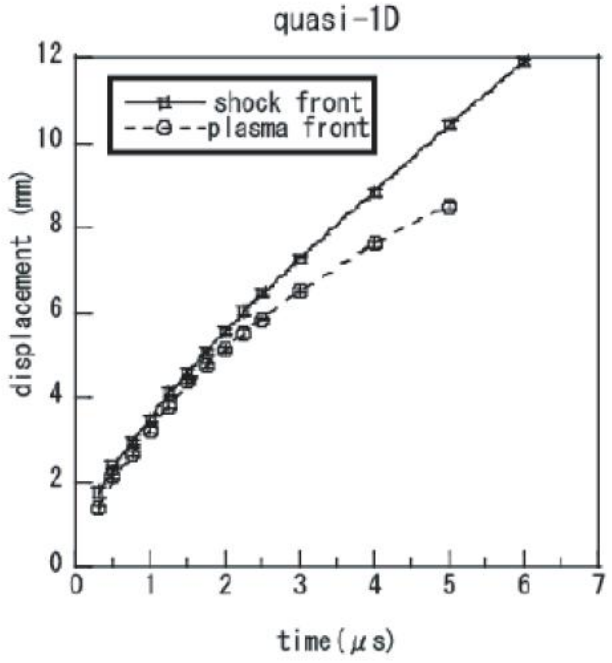

Fig.1.13 Propagation history of quasi 1-dimension laser plasma

Understanding important aspects of the structure of the laser-supported detonation wave is also important for designing vehicles. Shimamura, Hatai et al investigated the LSD internal structure such as the laser absorption layer thickness using two-wavelength Mach-Zehnder method. Furthermore, they measured the temperature of LSD wave using emission spectroscopy[21)]. The focusing set up of this experiment is same as Fig.1.9 (2-dimension experiment). The temporal and spatial distribution of the electron number density and the temperature are shown in Fig.1.14. The peak value of electron density was 2×10^{24} m^{-3} and the corresponding electron temperature was 30,000 K. From the result, the existence of the plasma ahead of the shock wave in the LSD regime was indicated.

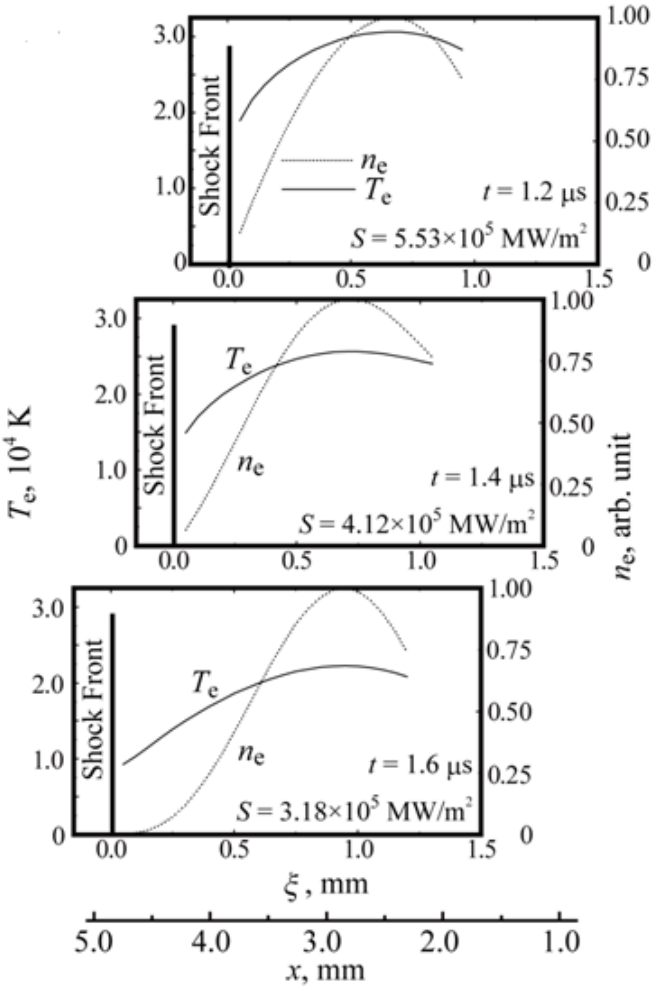

Fig.1.14 Temporal and spatial distribution of the T_e and n_e behind the shock wave front

1.5 Objectives

As noted above, during the period the LSD regime exists, the energy conversion process remains. However, when it terminates and transits to the LSC regime the conversion process is stopped. Hence, the shape of the laser propulsion vehicle is needed to keep the LSD regime longer.

Therefore, it is important to elucidate the LSD termination condition as it is still not clear. Now, the precise physics model of the LSD is not established. Shimamura, Hatai et al research results indicate the existence of the plasma in front of the shock wave but its result is not enough to establish it. To discuss the LSD termination in a more detailed manner, it is important to know the LSD structure visually and more exactly.

Hence from the above, the objectives of this research are defined as below:

- To pick up the exact LSD structure visually using HSHS method
- To evaluate the preceding plasma region quantitatively
- To investigate the energy dependency of the LSD structure
- To suggest the new LSD model

CHAPTER 2
Measurement of the shock and the ionization front by HSHS method

2.1 Half Self-emission and Half Shadowgraph method

In previous studies about laser plasma, they employed the traditional Shadowgraph method to get laser plasma image[15,22]. However, this method cannot detect the ionization wave front and shock wave front particularly, especially at earlier time of LSD propagation.

The Half Self-emission and Half Shadowgraph (HSHS) method can obtain the image of shock front and ionization front of the same laser induced plasma at the same particular time. The detail of Half Self-emission and Half Shadowgraph (HSHS) method is discussed below.

The schematic of the HSHS system set up is shown in Fig.2.1. Fundamentally, it is almost the same as the traditional Shadowgraph system. In this system, a shadow mask is located upstream of the probe light, and a band pass filter is located downstream of the probe light. Therefore with HSHS, half upper part, the self-emission image of laser induced plasma is obtained, and in half lower part, the shadowgraph image is obtained. The laser plasma is axially symmetrical, thus detailed discussion about the interaction of both fronts is achievable by comparing these two images.

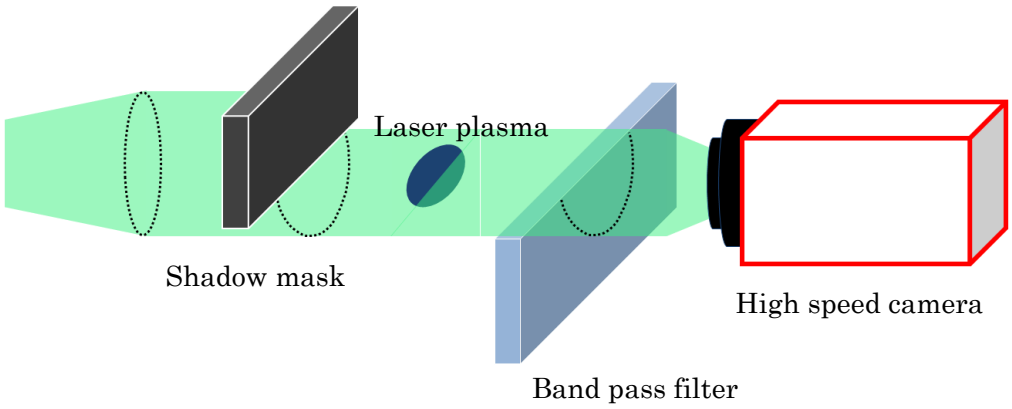

Fig.2.1 Schematic of the HSHS set up

2.2 HSHS experimental set up

The schematic of experimental set up is shown in Fig.2.2. Synchronization between the breakdown and the photographing is controlled by a delay generator, which first receives a trigger signal from the TEA-CO_2 gas laser, after adding a delay, it triggers the camera.

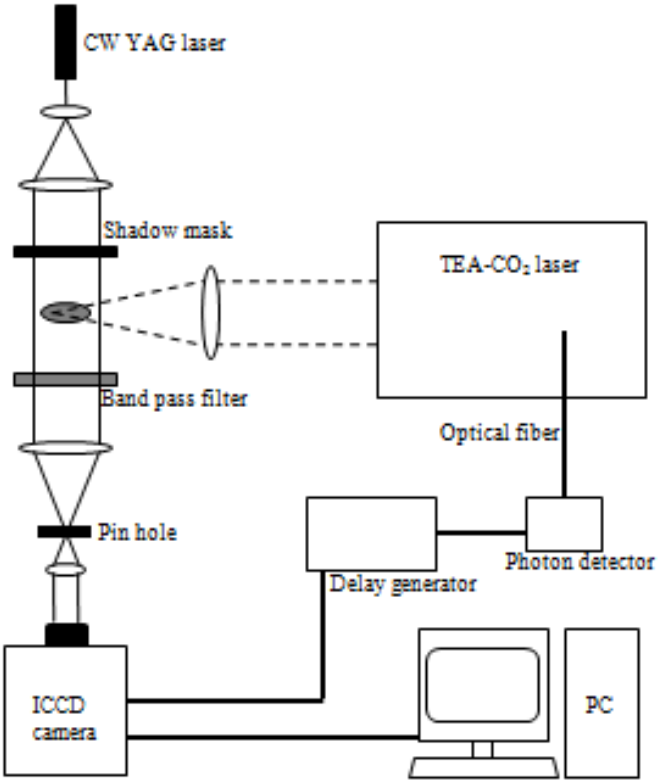

Fig.2.2 Schematic of experimental set up

2.2.1 Laser plasma generation part

TEA-CO_2 laser

In this study, the pulsed TEA-CO_2 Laser (transversely excited atmospheric pressure –CO_2 laser, Usho Co., Ltd., IRL-1201, λ = 10.6 μm), which can shoot 10 J pulsed laser beam at maximum charge was used. The laser beam pulse shape of 10 J is shown in Fig.2.3. The image of the laser burn pattern and the energy space distribution are shown in Fig.2.4. The schematic of the laser internal circuit and the photo image of the laser used are shown in Fig.2.5 and Fig.2.6 respectively.

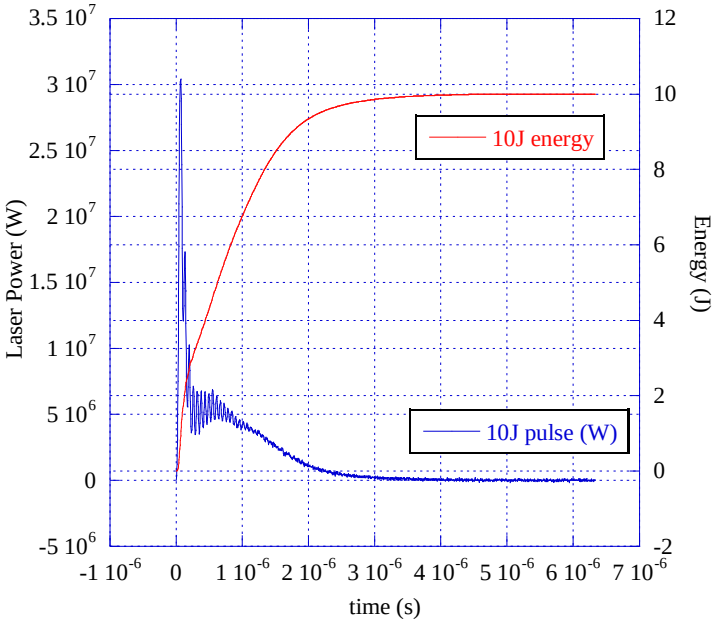

Fig.2.3 Laser pulse shape of 10 J

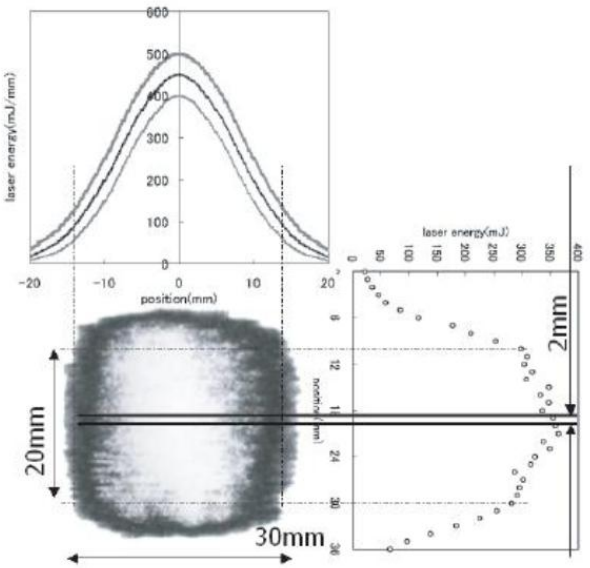

Fig.2.4 Laser burn pattern and energy space distribution

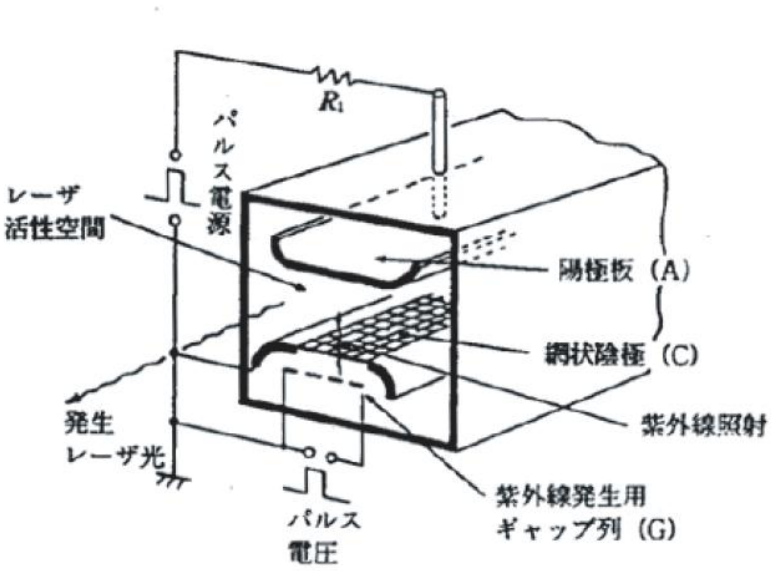

Fig.2.5 Laser internal circuit

Fig.2.6 Photo image of the TEA-CO2 laser

Collecting lens

In this study, in order to induce plasma, the ZnSe plane-convex lens (Ophir Co., Ltd.) was used. The f-length of this lens is 7.5 in and 2.5 inches in diameter. The image of lens is shown in Fig.2.7. From previous study, it has been shown that the larger the f-number of lens, the longer the LSD regime[15]. To keep the LSD regime long, we performed the experiment at a larger f-number condition compared to the previous study. In this study, the f-number is 6.35. The result of ray tracing of this lens is shown in Fig.2.8. From Fig.2.8, the beam width is collected to 0.05mm.

Fig.2.7 Collecting lens (ZnSe-lens)

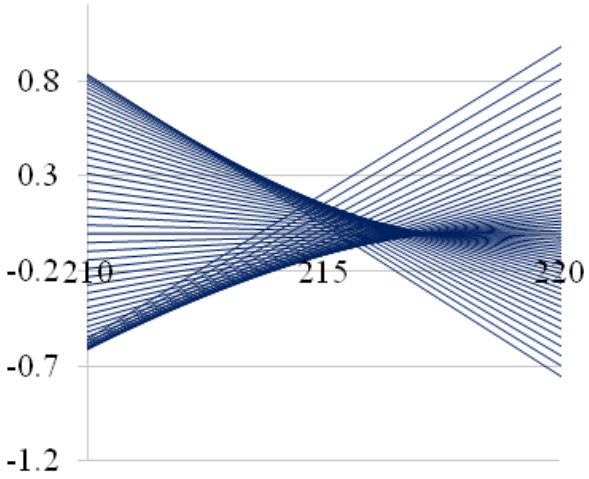

Fig.2.8 Result of ray tracing

2.2.2 Plasma observation part

High Speed Camera

In this study, to obtain the HSHS image, a high-speed intensified charge-coupled device (ICCD) camera (DRS technology Co., Ltd.) was used. This can take eight frames in each operation at the maximum framing rate of 100 million FPS with minimum exposure time of 10 ns, which can be controlled.

The flash from the gap switch of internal circuit in the TEA-CO_2 laser is used as the trigger for the shutter of the high speed camera. This trigger flash is detected by a photon detector and sent to a delay circuit. The delay circuit delays the signal and sends a TTL signal to the high speed camera.
The picture of the high-speed ICCD camera is shown in Fig.2.9.

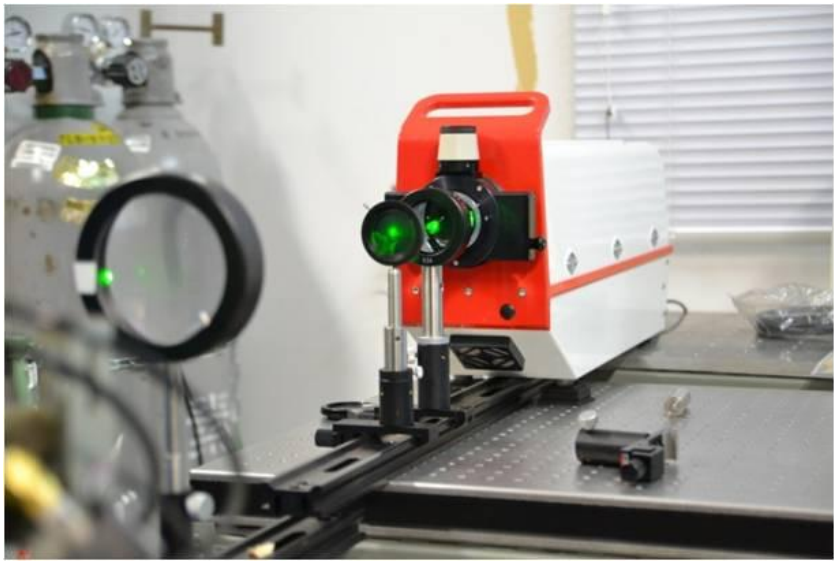

Fig.2.9 Ultra8, High speed ICCD camera

Probe Laser for Shadowgraph

A continuous wave yttrium aluminium garnet laser (λ = 532 nm) with 8 mW output power was used as a probe light. It projects the shadow of a blast wave on to the high-speed ICCD camera. In this study, the probe light was contracted by two convex lenses, f-length 700 mm and 250 mm at downstream and conducted to the high speed camera.

Band pass filter

For the shadow graph image, a band pass filter which can allow a 532 nm ± 2 nm wavelength light through it was used (CVI MellesGriot, XLL-532.0-2.00-DCUT, Fig.2.10). This represents the shock wave in shadow graph image clearly.

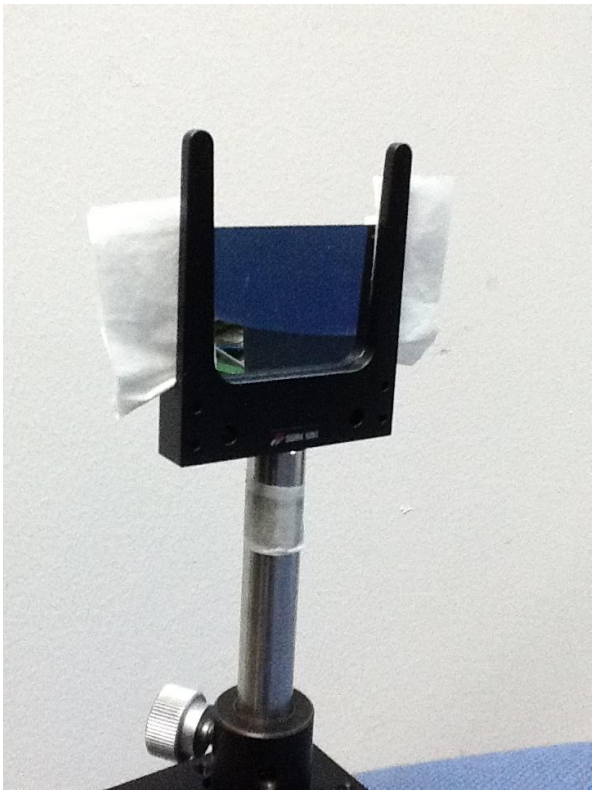

Fig.2.10 Band pass filter

2.3 Analysis method

The typical HSHS image is shown in Fig.2.11 as an example. We measured the intensity of brightness of the HSHS image: the shadowgraph part and the self-emission part accordingly. The distribution of the brightness was measured with a free/ public domain image analysis software called ImageJ. The measuring line is indicated by arrows in Fig.2.11. The distributions of the intensity of brightness of both images are shown in Fig.2.12 as an example. In Fig.2.12, the shock wave front position and the ionization wave front position are indicated as well.

To fix the shock wave front position, an initial rise point from the background brightness of the distribution was defined as the front. The initial rise is that large gradient completely absented from the noise. In a similar way to fix the ionization wave front position, an initial depression point was defined as the front.

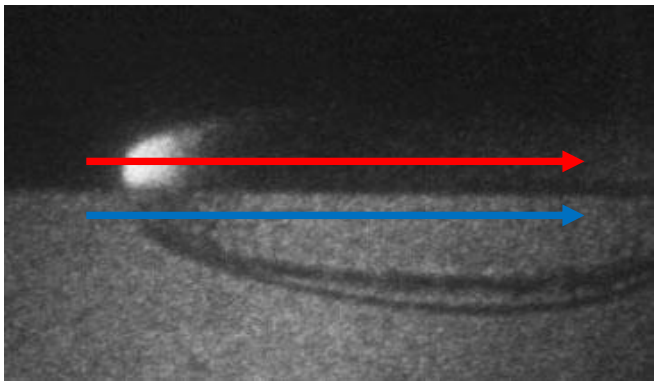

Fig.2.11 HSHS image

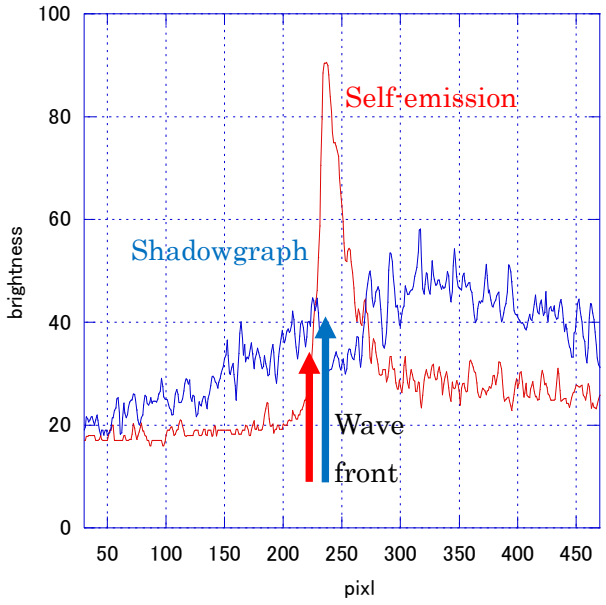

Fig.12 Distributions of brightness intensity of HSHS image

2.4 Experimental condition

In this study, the laser induced plasma was generated in Air at 100 kPa by TEA-CO_2 laser with incident energy of 7 J and 10 J. The laser beam was focused by ZnSe-lens whose f-length is 7.5 in.
In this experiment, the laser beam sustainability was verified by measuring the energy using a calorie meter, before and after the experiment. The variability was in 5 % of the energy. And the repeatability of the laser pulse shape was also confirmed by measurement using a photon drag detector (Hamamatsu photonics Inc.).

CHAPTER 3
Result and Discussion

3.1 Result of Experiment

In this section, the results of the experiment (7J, 10J) are described. In Fig.3.1 typical images of HSHS are shown as examples. In Fig.3.1 the incident laser beam line and a break down point are noted simultaneously.

On the image, the shock wave and the ionization wave are photographed individually. The half upper part shows the self-emission (the plasma ionization wave) image and the half lower part shows the shadowgraph (the shock wave) image. As noted from Fig.3.1, at the earlier time, a blast wave travels along the laser light channel in the direction opposite to the beam incidence.

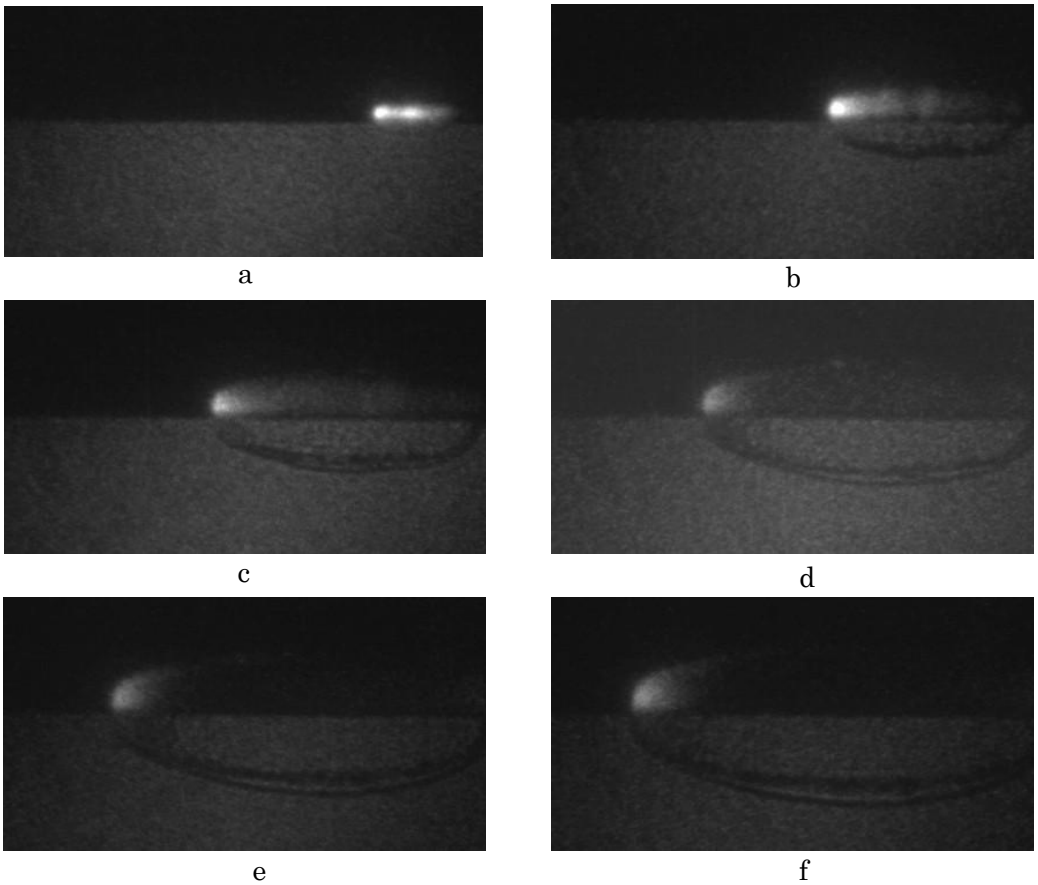

Fig.3.1 Typical images of HSHS

(a breakdown, b 500ns,c 1000ns, c 1500ns, d 2000ns, e 2500ns, f 3000ns)

3.1.1 Experimental result of 7J, Air

The laser induced plasma generated in Air by 7 J TEA-CO_2 laser was measured. The typical image of 7 J HSHS experiment during LSD is shown in Fig.3.2 as an example.

The incident laser power profile and the time variation of the cumulative energy of 7 J are shown in Fig.3.3. The horizontal axis indicates time (s), the left vertical axis is laser power (MW) and the right vertical axis is cumulative energy (J).

From images like Fig.3.1, the ionization wave front position and the shock wave front position were fixed by measuring the brightness intensity distribution. Then the distance from the break down point was measured and both wave front propagation histories were drawn. The wave front propagation histories are shown in Fig.3.4. Fig.3.4 shows result of 7 J experiment: the horizontal axis shows the time from break down (ns) and the vertical axis shows the distance from the break down point (mm). As shown in the result, the LSD termination time was around 2.9 μs from the break down.

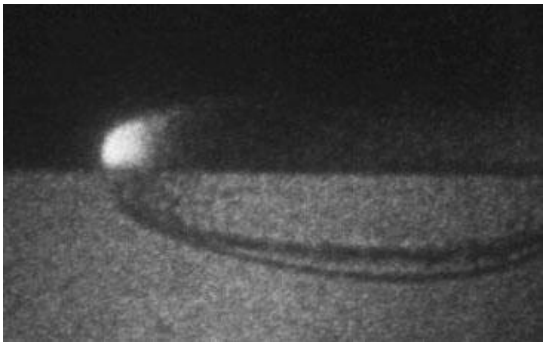

Fig.3.2 Typical image of HSHS 7 J

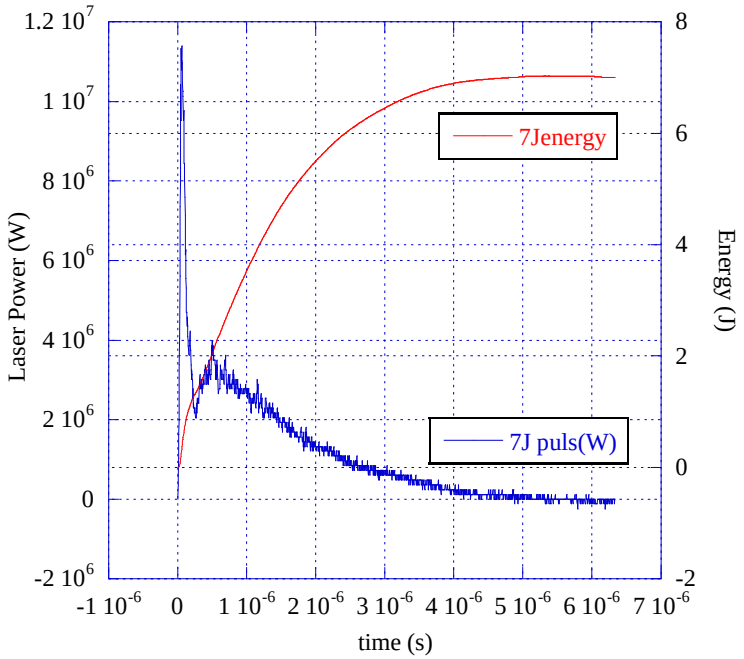

Fig.3.3 Energy profile 7J

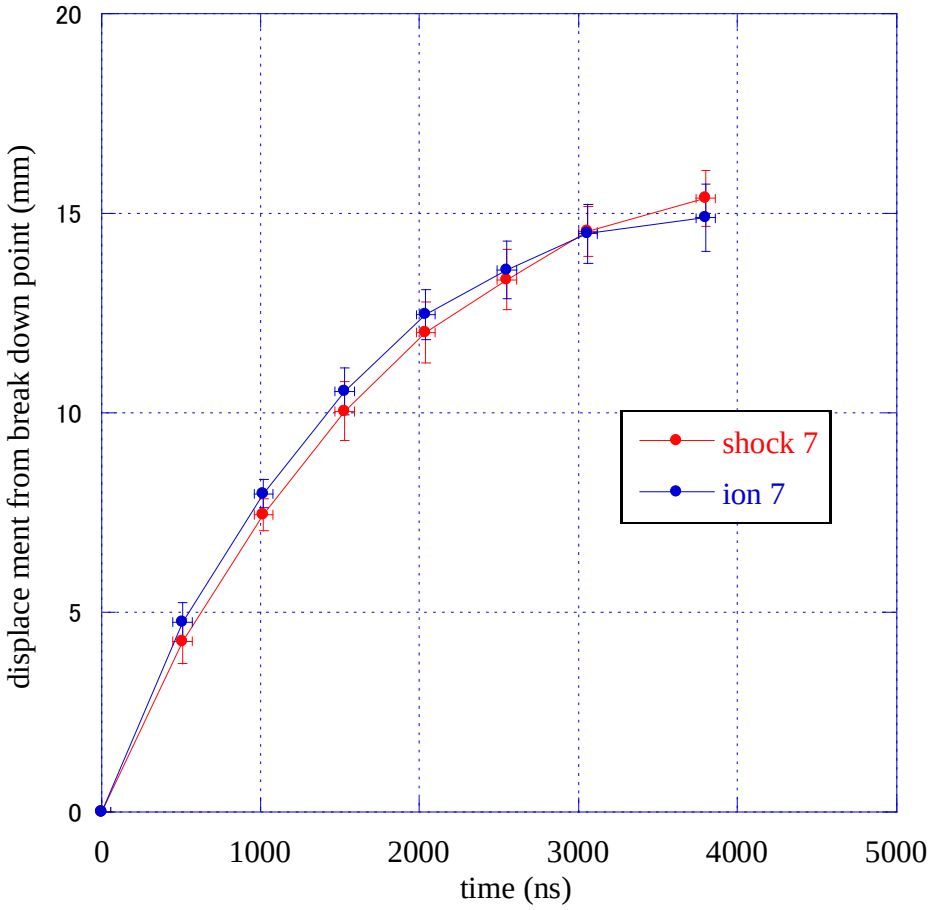

Fig.3.4 Ionization wave and shock wave propagation history 7 J

3.1.2 Experimental result of 10J, Air

The typical image of 10 J HSHS experiment during LSD is shown in Fig.3.5 as an example. The incident laser power profile and the time variation of the cumulative energy of 10 J are shown in Fig.3.6. The horizontal axis indicates time (s), the left vertical axis is laser power (MW) and the right vertical axis is cumulative energy (J).

The wave front propagation histories are shown in Fig.3.7. Fig.3.7 shows result of 10 J experiment: the horizontal axis shows the time from break down (ns) and the vertical axis shows the distance from the break down point (mm). As shown in the result, the LSD termination time was around 4.5μs from the break down. This trend where the LSD time is longer for higher incident laser energy is reported in other researches[15,22].

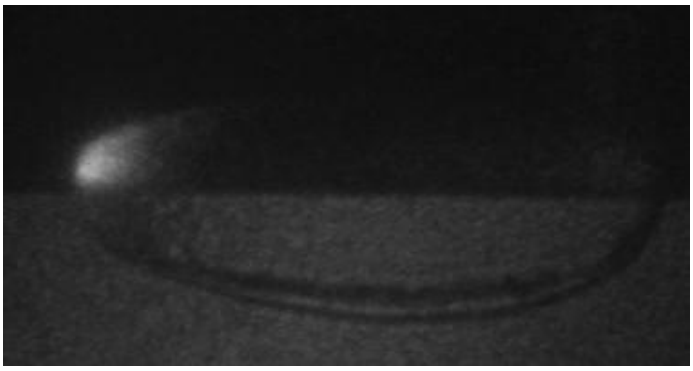

Fig.3.5 Typical image of HSHS 10 J

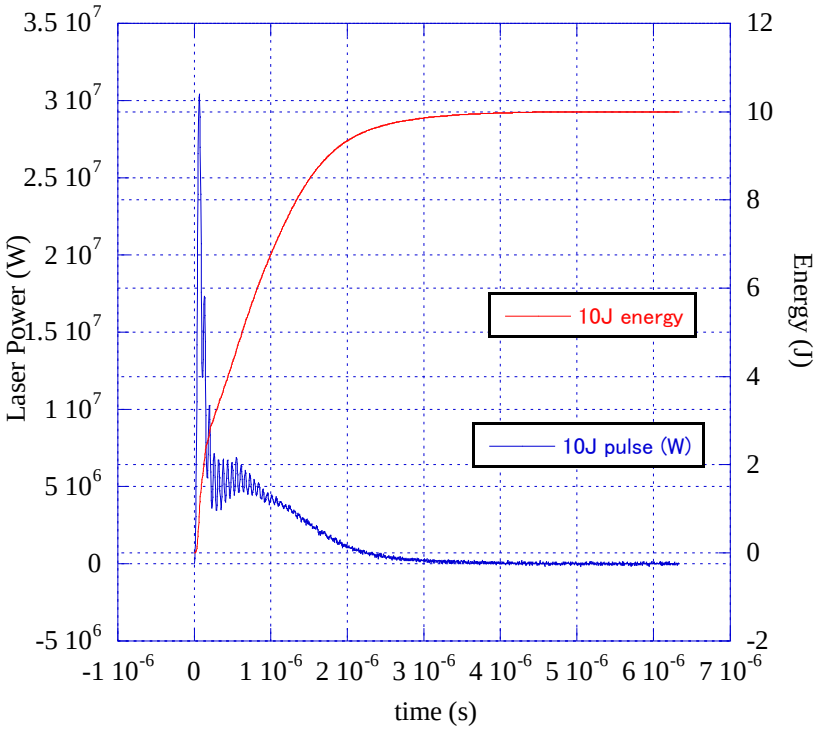

Fig.3.6 Energy profile 10 J

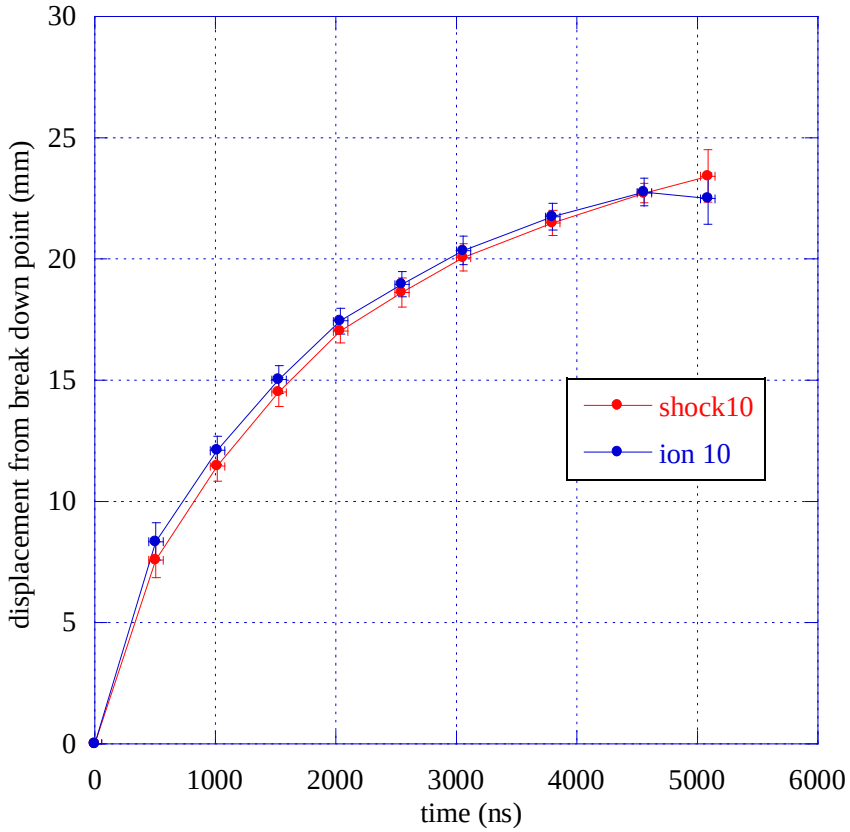

Fig.3.7 Ionization wave and shock wave propagation history 10 J

3.2 Shock wave inductive distance measurement

From the propagation history, in order to discuss the structure of LSD, the front difference, the shock wave inductive distance, was measured. In this study, the shock wave inductive distance is the difference in distance between the ionization wave front and the shock wave front measured from the point of break down.

3.2.1 Result of 7 J, Air

In Fig.3.8, the time variation of the shock wave inductive distance from the time break down occur of the 7 J experiment is shown. The horizontal axis shows the elapsed time from breakdown and the vertical axis shows the value of the shock wave inductive distance. In this graph, if the value is positive, it indicates that the ionization wave front is ahead of the shock wave front. Conversely, if the value is negative, it indicates that the ionization wave front is behind the shock wave front. From the result, the preceding plasma region exists during LSD regime. That region has a thickness of about 0.5 mm from the shock front.

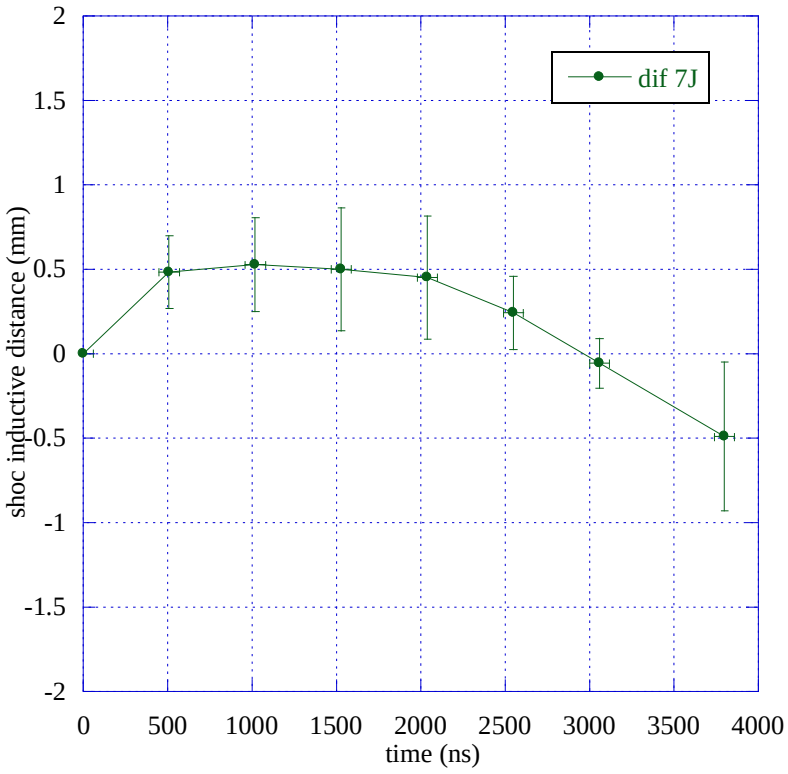

Fig.3.8 Time variation of shock inductive distance
from break down of 7 J experiment

3.2.2 Result of 10 J, Air

In Fig.3.9, the time variation of the front difference from the time break down occur of the 10 J experiment is shown. This figure's axes are same as Fig.3.8. From the result, the preceding plasma region also exists during LSD regime, just as was observed for the 7 J experiment.

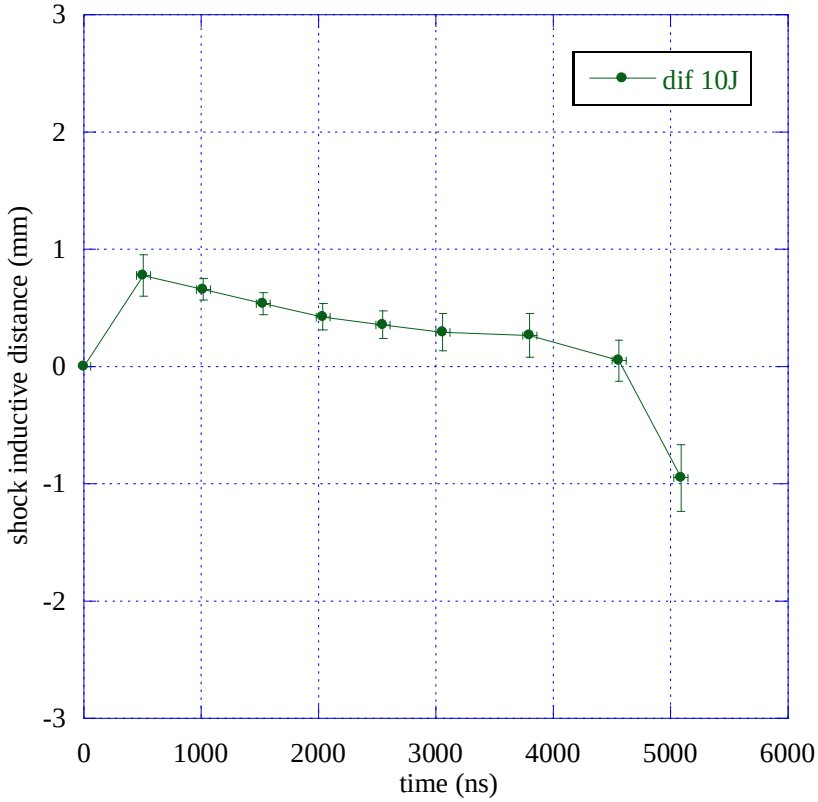

Fig.3.9 Time variation of shock inductive distance
from break down of 10 J experiment

3.3 Discussion on Energy dependence

The propagation history and time variation of wave the shock inductive distance compared with 7 J result and 10 J result are shown in Fig.3.10 and Fig.3.11 respectively. From Fig.3.11 each result shows that the plasma region existed during the LSD regime. This indicates that the LSD is a plasma induced phenomena.

Traditionally, the LSD structure is thought to be similar to ZND model of chemical detonation. In fact, it is known that the shock wave goes ahead whiles the reaction and heating region (plasma region) follows it by a reaction-induced distance. However, from the perspective of our experiment, the LSD structure is such that the laser heating region (preceding plasma region) goes ahead and the pressure wave (shock wave) is induced concomitantly. Despite the difference in value of the incident energy, the value of the preceding plasma region thickness is not so different. There is no change of structure.

In this study, the laser induced plasma was generated in Air by TEA-CO_2 laser. The thickness of the preceding plasma region could be influenced by ambient gas species, ambient gas pressure and incident laser wavelength etc. Therefore we recommend that further investigations via a detailed experimental analysis be carried out to determine the physical parameter that influences the preceding plasma region.

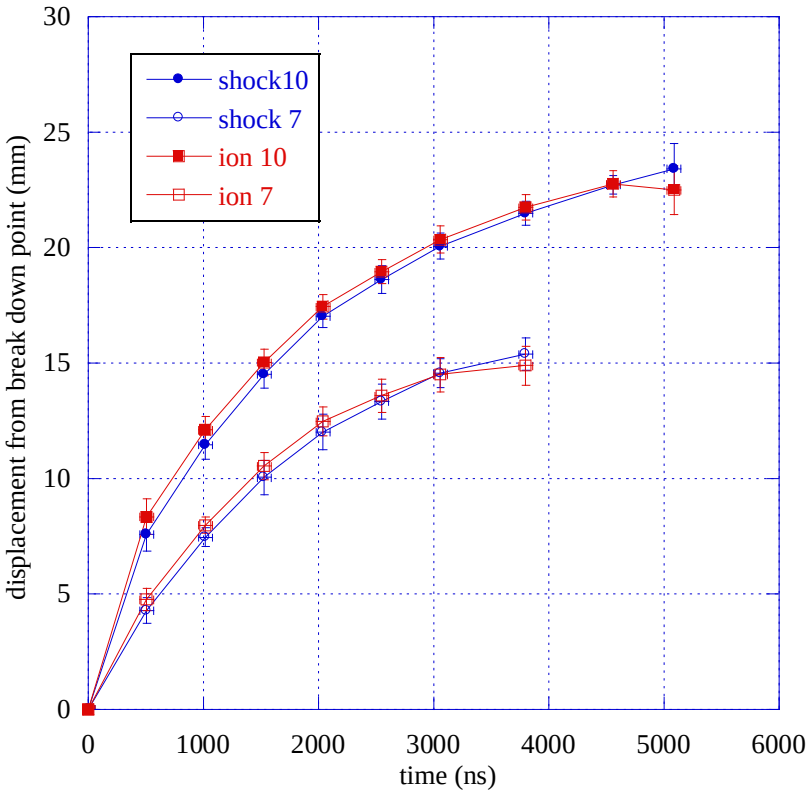

Fig.3.10 Energy comparison of propagation history

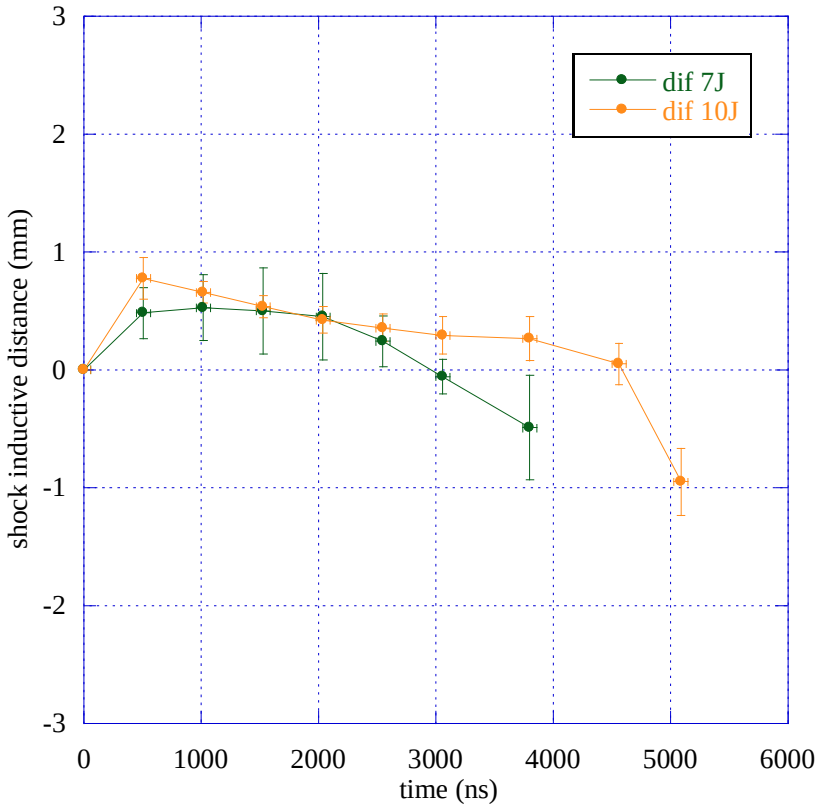

Fig.3.11 Energy comparison of shock inductive distance history

3.4 Oscillation of the shock wave inductive distance

In section 3.1 and 3.2, the time variation of the shock inductive distance was shown in some figure. However, that result is average of the multi experiments result. In this section, focus on the dynamics of the shock inductive distance of once experiment. In Fig.3.12, a time variation of the shock wave inductive distance of the once experiment.

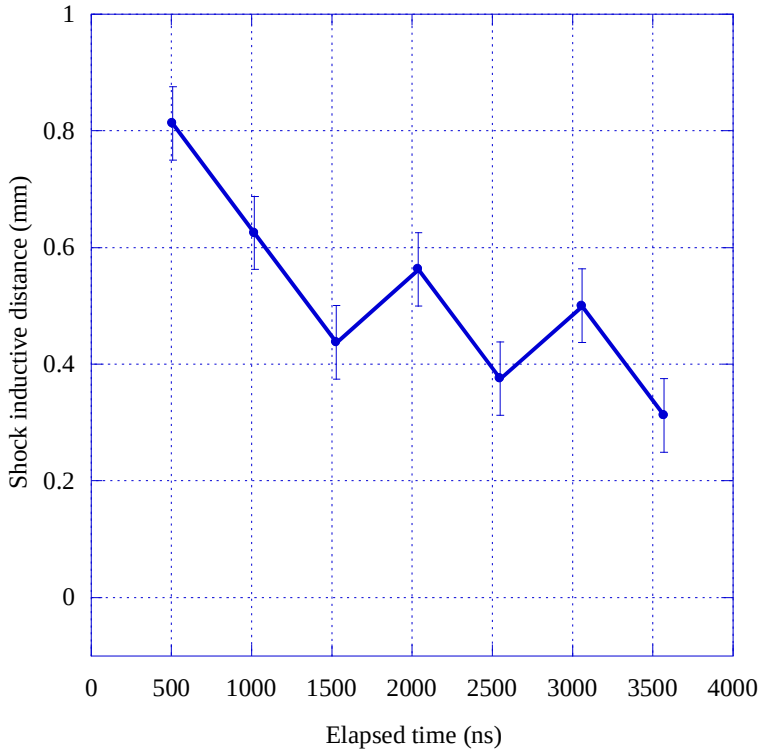

Fig.3.12 Time variation from break down of shock inductive distance (10J, 1 shot)

As the result, the value of the shock wave inductive distance was oscillated. Similar phenomenon is observed on the reaction inductive distance of the ZND chemical detonation. About ZND model, this phenomenon is caused by the shock wave and reaction region interaction[1)]. The ionization front and the shock wave front intend to keep suitable distance because of heat transport from a heating region to the shock wave. Thus the shock inductive distance oscillates.

3.5 New LSD model

In this study, the preceding plasma region was visualized by HSHS method. Then the region, a shock wave inductive distance, was evaluated quantitatively. As a result, it was identified that the shock wave inductive distance is about 0.5 mm during the LSD regime. Our research team has been researched on the LSD structure over the past several years.

The research for the electron number density in the behind of the shock wave

Hatai et al investigated the LSD internal structure such as the laser absorption layer thickness using two-wavelength Mach-Zehnder method[23]. In their research, the laser plasma was induced by line focused laser using 10J TEA-CO_2laser. From the result, the value of number electron density is about $10^{23}m^{-3}$ at the shock wave front. And it is about $10^{24}m^{-3}$ at the peak value of the distribution in the back of the shock wave. After this, the value decrease with distance from the peak because of attachment or recombination. In addition, they evaluate a laser energy absorption layer length in back of the shock wave. From the result, the length of absorption layer is about 0.2mm during LSD regime sustained from the shock wave to the peak of the electron number density distribution. The LSD structure is nearly independent of the size of laser plasma, so the electron number density of the laser plasma generated in present study is almost same as previous.

The research for precursor region in front of the LSD wave

The LSD wave is a phenomenon that the plasma ionization wave propagates at supersonic. In streamer discharge, there is similar phenomenon. In the streamer theory, it is necessary to sustain the propagation of the plasma ionization wave that a region called precursor is generated in front of the ionization wave. In this region, some seed electron is generated by VUV radiated from plasma layer. The seed electrons generated in the precursor region induce an electron avalanche. The electrons increased by electron avalanche consists the new plasma layer, so the propagation is sustained.
In 2010, we researched on the precursor region of laser plasma. In this study, the laser plasma was induced by glass laser and TEA-CO_2 laser[24]. The electron temperature and number density was measured. Then the photon emission intervals at LSD termination time were estimated. As the result, it was confirmed that the precursor region is necessary to sustain the propagation of LSD same as the streamer propagation.

As described above, in the previous researches, the structure of in front of LSD wave and in back of shock wave of LSD were discussed. The shock wave inductive distance measured in present study is the region between those two regions. These result and the result of this study was summarized and a new LSD structure model is proposed. The new LSD structure model is shown in Fig.3.13.

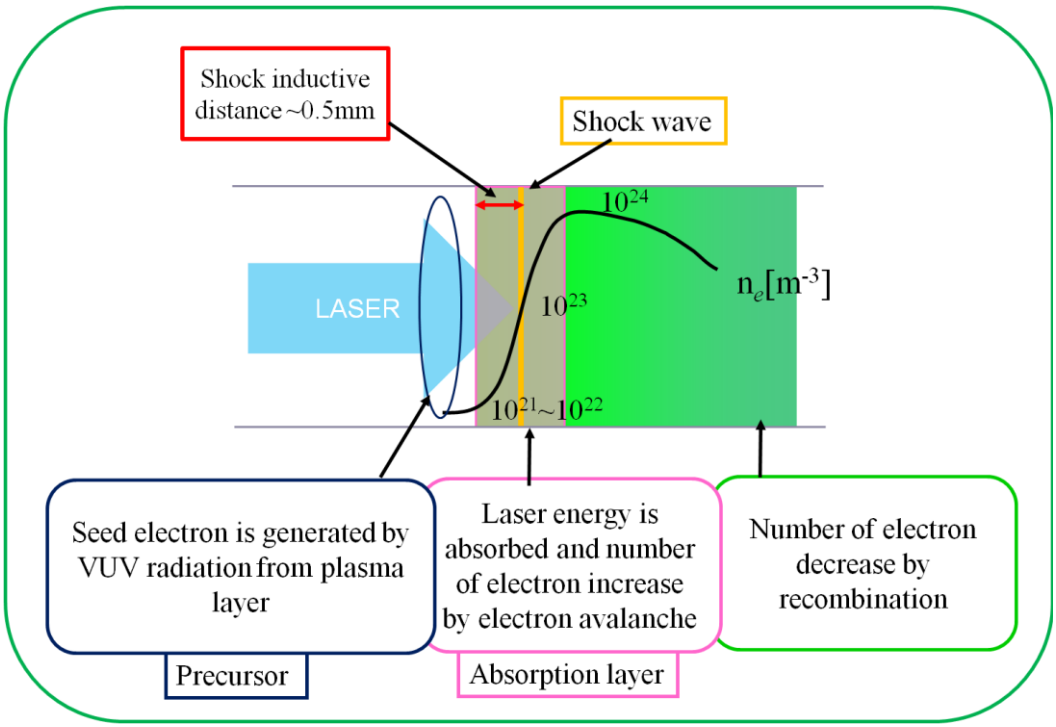

Fig.3.13 New LSD model

Some features follow.

- In front of the LSD wave front, there is the precursor region where the seed electrons generated by the VUV radiation from the plasma layer in the LSD wave.
- The shock wave inductive distance is from the point, where the electron number density is over 10^{21}~$10^{22}m^{-3}$ and the inverse bremsstrahlung becomes pronounced, to the shock wave front. And its value is about 0.5mm on average.
- Actual value of the shock wave inductive distance is oscillated.
- At the shock wave, the electron number density is about $10^{23}\,m^{-3}$. The electron number density is about $10^{24}m^{-3}$ at the peak in back of shock wave. After the peak, the recombination becomes pronounced and the electron decrease.
- In the back of the shock wave, the length of the laser energy absorption layer is about 0.2 mm and its ends ahead of the shock wave. The absorption layer is about almost 1mm including the shock wave inductive distance and the shock wave is in the absorption layer.

CHAPTER4
Conclusion

The structure of the laser induced plasma was investigated by Half Self-emission Half Shadowgraph method. The laser induced plasma was generated in Air by the TEA-CO_2 laser at 7 J and 10 J respectively. The focal length was 7.5 in. From the image, the brightness intensity distribution was measured and the positions of the ionization wave front and the shock wave front were fixed. As the result showed, the wave front propagation history from break down point was drawn and the time variation of the difference between ionization wave front and shock wave front was measured.

From the propagation history, the LSD termination times of 7 J experiment and 10 J experiment are around 2.9 μs and around 4.5μs respectively. From the measurement of difference of wave front, it is shown that the preceding plasma region exist in front of the shock wave front. The shock wave inductive distance is about 0.5 mm despite the difference in incident energy. And a new LSD structure model is proposed by summarizing researches on the LSD structure.

In conclusion, the LSD structure is not similar to the ZND model of chemical detonation. The shock wave inductive distance is thought to be necessary to keep the LSD regime. In fact the LSD is a plasma induced phenomena and the thickness of the preceding plasma region is independent of the value of the incident energy.

Appendix

In addition to research content described in a body text, to investigate the influence of ambient gas species on the shock inductive distance, the laser plasma induced in Nitrogen and Argon gas was observed. In Fig.1, the experiment set up is shown.

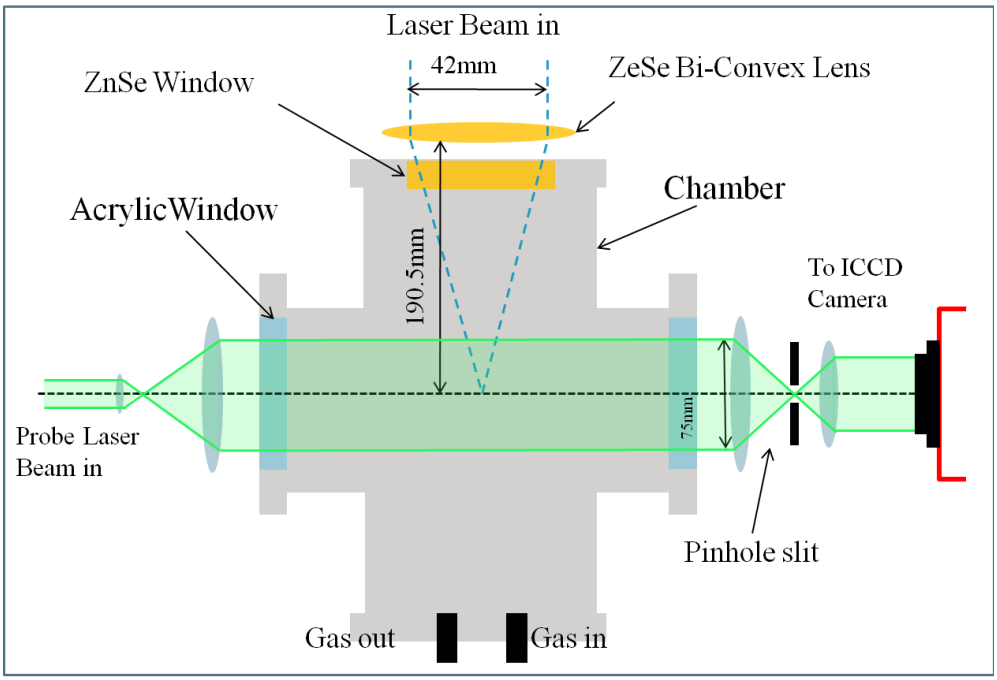

Fig.AP.1 Experimental set up for N_2 and Ar experiments

The HSHS images of Nitrogen and Argon were shown in Fig.2 Fig.3as examples respectively.

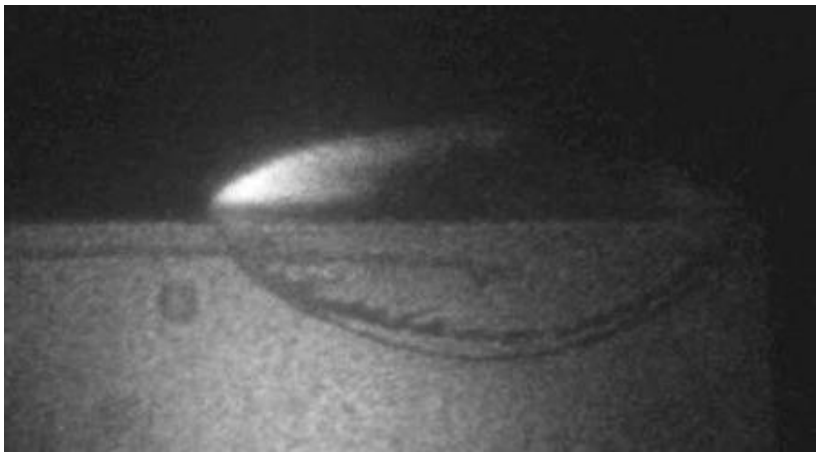

Fig.AP.2 HSHS image of laser plasma in N_2

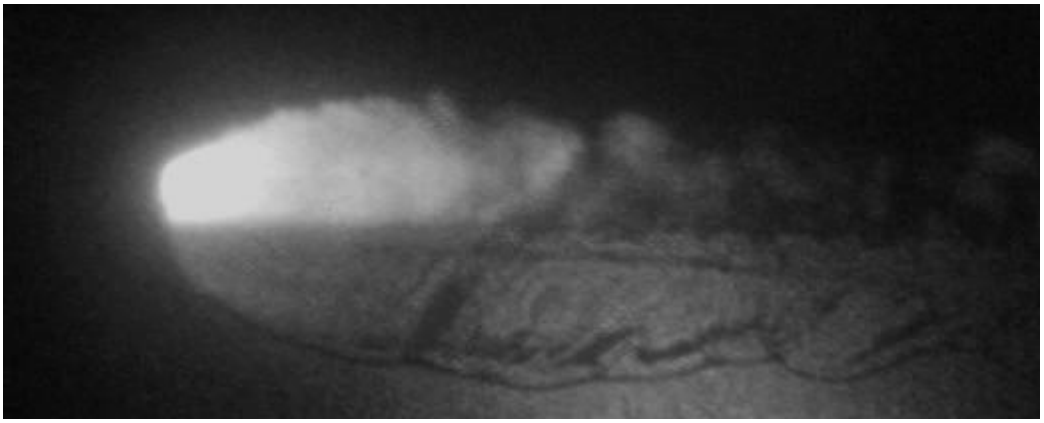

Fig.AP.3 HSHS image of laser plasma in Ar

The shock inductive distance time variation and propagation history of the laser plasma generated in Nitrogen were shown in Fig.4 and Fig.5, respectively.

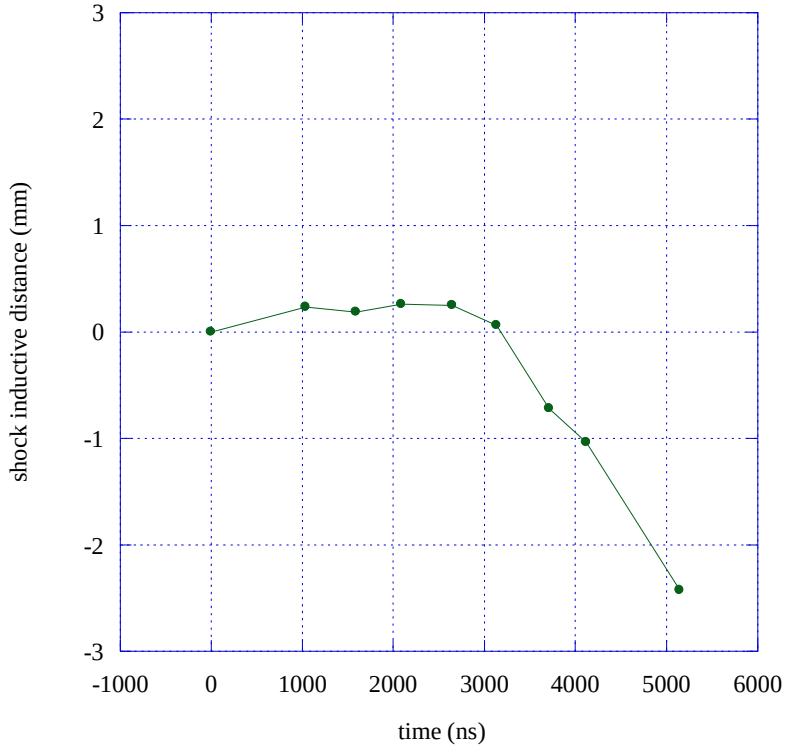

Fig.AP.4 Time variations from break down of shock inductive distance of N_2

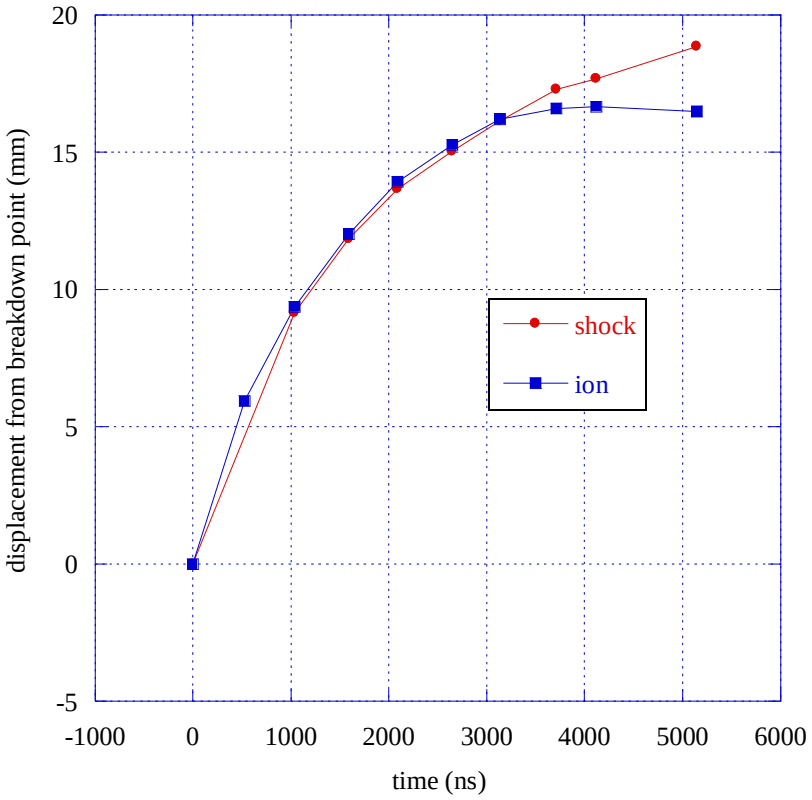

Fig.AP.5 Ionization wave and shock wave propagation history of N_2

From the result of the Nitrogen experiment, the shock inductive distance was about 0.2 mm. About Argon, the distance is thought to be over 0.5 mm. This is thought the shock inductive distance is influenced by ionization energy of gas species. And it is thought that the laser absorption layer length including the shock wave inductive distance increase in order of ionization energy from low to high. However, about effect of gas species, more detail investigation is needed.

Reference list

1. Kantrovitz, A. “Propulsion to Orbit by Ground Based Lasers,” *Aeronautics and Astronautics*, vol.10, 1972, pp. 74-76
2. Raizer, Y. P., “Laser-Induced Discharge Phenomena,” pp.199-204, 1972
3. Pirri, A. N., Schler, R., and Northam, D., “Momentum transfer and plasma formation above a surface with a high-power CO2 laser”, Applied Physics Letters, Vol. 21, 1972, pp.79-81.
4. Simons, G. A., “Momentaum Transfer to a Surface When Irradiated by a High-Power Laser”, AIAA Journal, Vol.22, 1984, pp.1275-1280.
5. Simons,G.A., and Pirri,A.N.“The Fluid Mechanics of Pulsed Laser Propulsion”,AIAA Journal, Vol. 15, 1977, pp.835-842.
6. Pirri,A.N,and Monsler,M.J.,”Prpulsion by Absorption of Laser Radiation”, AIAA Journal, Vol. 12, 1974, pp.1254-1261.
7. Ageev,V.P.,Barchukov,A.I,Bunkin,F.V.,Konov,V.I.,Korobeinikov,V.P.,Putjatin,B.V.,andHudjakov,V.M., ”Experimental and theoretical modeling of laser propulsion”, Acta Astronautica, Vol. 7, 1980, pp.79-90.
8. Myrabo,L.M.,Messitt,D.G.,and Mead,Jr.,F.B.,”Ground and Flight Testsof Laser Propelled Vehicle”,AIAA Paper 98?1001,1998
9. Sasoh,A.,”Laser-Propelled Ram Accelerator,”*Journal of physics IV France*,Vol.10,2000,pp41-47.
10. Zel’dovich, Y. B., and Raizer, Yu, P., “Physics of Shock waves and High-temperature Hydrodynamics Phenomena,” Dover, NewYork, 2002,
11. L. J. Radziemski, D. A. Cremers, Laser-Induced Plasmas and Applications, *CRC Press*, New York, 1989
12. Fischer, V. I., Soviet Physics: Technical Physics, Vol.28, 1984
13. Jumper, E. J., Physics of Fluids, Vol.21, 1978, p.549.
14. Nielsen, P. E., “Hydrodynamic calculations of surface response in the presence of laser-supported detonation waves,” Journal of Applied Physics, Vol. 46, 1975, pp. 4501-4505.
15. Mori, K., Komurasaki, K. and Arakawa, Y., “Influence of the Focusing f Numberon the Heating Regime Transition in Laser Absorption Waves,” J. of Appl.Phys.15, (2002), pp.5663-5667
16. Mori, K., Komurasaki, K. and Arakawa, Y., “Energy Transger from a Laser Pulse to a Blast Wave in Reduced-Pressure Air Atomospheres,” J. of Appl. Phys. 95, (2004), pp.5979-5983.
17. Bohn, W. L., and Schall, W. O., “Laser Propulsion Activities in Germany” in *Proceedings of First International Symposium on Beamed Energy Propulsion* (*AIP Proceedings*, Vol. 664) ed. By A. V. Pakhomov, 2003, pp. 79-91
18. Sasoh, A., Kister, M., Urabe, N., and Takayama, K., “Laser-Powered Launch in Tube,” *Transaction of Japan Society of Aeronautical and Space Sciences*, Vol.46, 2003, pp. 52-54.
19. 福田章雄, “干渉法によるポストレーザー支持爆轟波の特性解明,” 東京大学修士論文
20. 牛尾正人, “Characteristics of Line Focused Laser Supported Detonation,” 東京大学修士論文
21. K. Shimamura, K. Hatai, K. Kawamura, A. Fukui, B. Wang, T. Yamaguchi, K. Komurasaki, and Y. Arakawa, Internal Structure of Laser Supported Detonation Waves by Two-Wavelength Mach-Zehnder Interferometer, *J. Appl. Phys.*, Vol.**109**, 2011, 084910

22. Wang. B., Komurasaki. K., Yamaguchi. T, and Shimamura. K, Energy conversion in a Glass-laser-induced blast wave in air, *J. Appl. Phys*. Vol. 109, 084910, (2011)
23. 畑井啓吾, ”レーザー支持爆轟派の加熱構造とその維持条件,” 東京大学修士論文
24. K. Shimamura, K. Michigami, K. Komurasaki, B. Wang, Y. Arakawa, Effect of laser wavelength on Laser Supported Detonation using spectroscopic techniques, Applied Plasma Science, 19, pp.17-22

Conference and Paper

- Conference

  "レーザー支持爆轟波の伝播構造における気体種依性" レーザー学会学術講演会第 31 回年次大会,,調布，2011 年 1 月

  "レーザー支持爆轟波性能の f 値及び気体種依存性", 第 51 回航空原動機宇宙推進講演会, JSASS 2011-002,広島市,2011 年 3 月

  “Influence of Gas Species on LSD Dynamics”, 28th International Symposium on Space Technology and Science, 2011-b-42s, Okinawa, JPN, June 2011

- Paper

  “HSHS 撮像法によるレーザー支持爆轟波構造の解明”, 応用プラズマ科学

Acknowledgments

本論文を書くにあたり，多くの方々に御世話になりました.
直属の指導教官である小紫公也教授には研究生活全般にわたるご指導を頂きました．日々の研究輪講会やディスカッションはもとより，最後の最後まで叱咤激励いただき，研究に対する考察を深めることができました．大変感謝しております，ありがとうございました．荒川義博教授には学会等で暖かい言葉を掛けて頂き，研究に躓いたときの心の支えの言葉になりました．小泉宏之准教授には輪講会で厳しいご意見を頂き，大変参考になりました．

小紫研究室に所属される諸先輩方にも大変感謝しております．山口敏和先輩には，研究に関するアイデアを共に考えていただき，研究結果の見せ方や発表方法などを教わり，発表の練習に深夜までお付き合いいただいたりと感謝がつきません．野村哲史先輩には実験器具の使い方を丁寧に教えていただきました．輪講などでも的確な質問，アドバイスで研究の疑問点，問題点を明らかにしていただきました．また，研究姿勢に大変感銘を受け，学ばされることが大変多くありました．同じ RP レーザー班であった，王彬先輩には未熟であった私に丁寧に実験方法を教えて頂きました．嶋村耕平先輩は初年度は共に研究を行い，修士二年以降の独立した研究生活をできるだけの力を付けさせていただきました．昨年度にマイクロ波伝送班に所属された小田章徳先輩には，学部時代から御世話になり，小紫研究室に所属するに当たり大変御世話になりました．

研究室の同期の方々とは日々励ましあい，支えあい，研究を進めることができました．ありがとうございました．柏キャンパスに所属する，石場舞さん，小松怜史くん，田中憲作くん，福成雅史くん，水野嘉祐くんには日々切磋琢磨しあえたこと，特に感謝しております．

また，研究室の後輩である，武市天聖くん，山川将人くんとは共に議論しあうことで研究に対する理解を深めることができました．

このほか，荒川・小紫・小泉研究室に所属され御世話になった全ての方々に，この場を借りて改めて感謝の意を表したいと思います．

柏キャンパスでの研究生活は大変厳しく苦しい時期もありましたが，多くのことを学び，多くの仲間と出会うことができました．この 2 年間で得たものを糧にこれからも精進し，航空・宇宙分野の発展に尽力していきたいと思います．

最後にここまで，支えてくれた錦野友太くんを代表する多くの友人，今日まで生活面，金銭面での援助とこのような人生を歩める環境を与えてくれた両親に大変感謝いたします．

本論文がレーザー推進の物理過程解明に多少とも寄与し，システム実現が一日でも早くなることがあれば，大変幸いに思います．